Case Studies in Thermal Engineering 18 (2020) 100610

Contents lists available at ScienceDirect

Case Studies in Thermal Engineering

journal homepage: http://www.elsevier.com/locate/csite

Numerical study of inlet air swirl intensity effect of a Methane-Air Diffusion Flame on its combustion characteristics

Amirjavad Ahmadian Hosseini [a], Maryam Ghodrat [b,*], Mohammad Moghiman [a], Seyed Hadi Pourhoseini [c]

[a] Department of Mechanical Engineering, Ferdowsi University of Mashhad, Mashhad, Iran
[b] School of Engineering and Information Technology, University of New South Wales Canberra, Canberra, 2610, ACT, Australia
[c] Department of Mechanical Engineering, University of Gonabad, Gonabad, Iran

ARTICLE INFO

Keywords:
CFD
Swirl number
Temperature
Radiation heat transfer
Nitrogen oxides (NOx)

ABSTRACT

In this paper, the effect of inlet air swirl number of a Methane-Air Diffusion Flame on dynamic flow behavior, temperature, and radiation heat flux distribution was investigated using ANSYS-Fluent CFD code. Based on the swirling effect on dynamic flow behavior, a specific equation in terms of axial and tangential velocity components was used to reach the swirl number. The modeling of the chemical reaction was carried out by applying the Eddy Dissipation Model (EDM). Furthermore, radiation heat flux and turbulent flow characteristics were performed by using P-1 and standard k-ϵ models.

The results showed that the elevating swirl number of the inlet air from 0.0 to 0.6 develops the furnace internal recirculation zone which leads to producing the combustion products in the internal recirculation zone. Consequently, fuel and air are mixed more efficiently, which results in the enhancement of combustion efficiency by removing the high-temperature zones as the leading cause of producing nitrogen oxides (NOx). Moreover, as the swirl number increases, the radial flow distribution improves, and the flame heat exchange area enhances regardless of the maximum flame temperature reduction, which will increase the flux radiation efficiency by 36.5% and reduces the pollutant NOx by 58.6%.

1. Introduction

Maximum efficiency of combustion and minimum pollutants' production are among the essential matters in combustion research. In this regard, combustion phenomenon and its influencing factors, such as the fuel/air ratio as one of the most critical factors in the flame formation, have attracted many researchers' attention [1,2]. Increasing the swirling rate of inlet airflow into the combustion chamber is an approach to enhance the fuel-air mixing rate in non-premixed combustion [3,4]. In non-premixed flames, increasing the swirling number increases the residence time of the combustion species inside the combustion chamber, which affects the flame temperature distribution, heat transfer rate of the flame, and pollutant formation [5,6]. Poorhoseini et al. [7] investigated the effect of enhancing the inlet air swirl number in liquid fuel burners. They found out that increasing the swirl number would reduce the emission of nitrogen oxides (NOx) and result in a lower exhaust temperature of the combustion chamber. Zhou et al. [8] studied the effect of the swirl number on the production rate of nitrogen oxides and perceived that as the swirl number increased, the mean flame temperature

* Corresponding author.
E-mail address: m.ghodrat@adfa.edu.au (M. Ghodrat).

https://doi.org/10.1016/j.csite.2020.100610
Received 2 January 2020; Received in revised form 13 February 2020; Accepted 18 February 2020
Available online 19 February 2020
2214-157X/

slowly rose, and the exhaust outlet temperature and the nitrogen oxide pollutants concentration decreased. Bashirnezhad et al. [9] studied the effect of swirl number on flame temperature and soot formation rate and noticed that by increasing the swirl number, the flame approached the burner inlet. They also found out that as the swirl number enhanced, the amount of soot in the combustion chamber decreased. In another study, Bonatesta et al. [10] studied the effect of the swirl number on the exhaust soot concentration, which showed that by elevating the swirl number to about 2, the concentration of exhaust soot emission declined, but with the increase of swirl number to values greater than 2, the exhaust soot concentration gradually boosted. Jerzak and Kuznia conducted an experimental study to determine the influence of changing the equivalence ratio and the atmospheric oxygen percentage of a methane diffusion flame on its flashback and blow-off at different swirl numbers. They concluded that by increasing the swirling number, a better range of flashbacks and blow-offs were observed in all of the equivalence ratios and oxidizing percentages [11]. Patel and Shah [12] conducted an experimental study to investigate changing air and fuel velocity effects on the appearance of a diffusion flame. They also examined the effect of swirling flow with various vane angles on the flame length and realized that inverse diffusion flames (IDFs) with swirling flow are shorter, wider, and more stable in comparison with those IDFs without swirling. In another experimental study, Patel and Shah studied the effect of hydrogen enrichment of natural gas diffusion flame in swirling and non-swirling state. They found out that in both cases, the addition of hydrogen decreased the flame length and raised its temperature. However, for a specific amount of mass based hydrogen addition, the non-swirling flame experienced much higher temperature increase than the swirling flame, which increased the rate of NOx pollutant generation in the non-swirling case [13]. Vakilipour et al. performed computational modelling to investigate the effect of carbon dioxide dilution on flame characteristics of a swirling diffusion flame; they understood that adding CO2 to the fuel stream caused the reduction of the flame length at all swirl numbers. However, with enhancing the swirl number, the flame length reduction rate was more remarkable [14]. In a numerical study, Keramida et al. [15] examined the effect of considering the radiation model in predicting the combustion characteristics of a methane/air turbulent diffusion flame. Two radiation models, including the discrete transfer model and six-flux model, were used for this purpose. They perceived that in regard to the radiation model, the predicted temperature distribution and the experimental data of Wilkes et al. [16] would be in good agreement. Furthermore, both of the radiation models provided acceptable results. When the radiation model was ignored, the temperature distribution in the furnace was over-predicted compared to experimental data. Khelil et al. [17] performed numerical modeling using the PDF combustion model coupled with the RSM turbulence model to predict the amount of NOx pollutants of a high swirling natural gas diffusion flame. They found out that the high-temperature zone revealed the flame formation in the central recirculation zone. Moreover, the highest level of NOx production rate was found in this region, and the lowest NOx level occurred in the low-temperature zone of the furnace. In another work Khanafer and Aithal [18] carried out a numerical study to investigate the effect of the swirl number on the combustion pollutants of a natural gas diffusion flame. In this simulation, they used the FIDAP commercial software; they inferred that increasing the swirl number improved the fuel/air mixing rate significantly, which eventually reduced combustion emissions. They disclosed that raising the swirl number reduced carbon monoxide and other unburned gases 3 to 5 times. Many researchers have investigated the combustion characteristics and emission of various liquid fuels with gaseous fuels in dual-fuel diesel engines [19]. They have found out that the NOx emission rate in gaseous fuels is significantly lower than that in liquid fuels. This significant difference in the NOx pollutants rate is due to higher heat capacity, lower oxygen content, and lower combustion temperature of gaseous fuels in comparison with liquid fuels [20]. In an experimental investigation, Yoon and Lee concluded that NOx emissions were significantly lower under dual-fuel operation than those in single fuel mode in each engine load conditions [21]. An experimental study on the emission and combustion characteristics of a dual fuel diesel engine has also been carried out by Mustafi and Raine [22]. Their study determined that, for the dual-fuel, NOx emission was always lower than diesel fuelling mode under the identical engine. In another study, Liu and his co-authors [23] showed that the dual-fuel mode presented a lower NOx emission rate than the diesel mode because most fuel was burnt at lean conditions resulting in lower local temperature, which caused lower NOx emissions.

Given the vital role of swirling in the air-fuel mixing rate and, consequently, the dynamic and combustion behavior of the flame [24,25], it is significant to determine the correct swirl number for modeling combustion flows.

In the present study, a novel equation based on the ratio of tangential and axial flow velocity components is used to determine the swirl number of the inlet air to the combustion chamber, and the results are compared with existing experimental data and similar numerical results. Also, since the effect of changing the inlet airflow swirling intensity on flame radiant heat transfer flux (as the primary mechanism of heat transfer from the flame) has rarely been investigated in the previous articles, the effect of flow swirl number on flame temperature and radiation heat transfer rate has also been studied and analyzed in this paper.

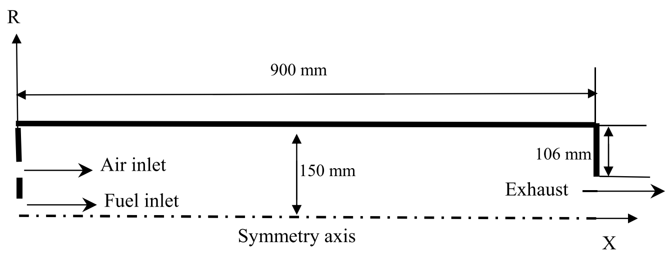

Fig. 1. Harwell combustion chamber geometry [26].

2. Mathematical model

The Harwell standard furnace [26] is used to investigate the effect of airflow swirling (changes of the swirl number) on the combustion characteristics of the methane-air flame, shown in Fig. 1. In this furnace, the fuel-air flow enters the combustion chamber in a two-dimensional, steady-state, and turbulent condition with velocities of 0.15 and 12.8 m/s and 295 K, respectively. Table 1 shows the operating conditions of the furnace. As reported by İlbaş et al. [27], The equivalence ratio for all of the swirl numbers in using the Harwell furnace is constant and equal to 0.83.

The finite volume method is utilized to solve the governing equations, including conservation of mass and momentum, energy conservation, turbulence equations, radiation, and species conservation equation. The SIMPLE algorithm is used to couple pressure and velocity equations. All equations are solved in the second-order upwind scheme, and the convergence limit is assumed when the residual values are less than10^{-6}.

Despite the increasing capabilities of numerical computing, researchers are keen to use simple combustion models that are highly precise, without high computational cost. These simple models are especially suitable for turbulent flow calculations for which the description of chemistry in detail is costly [28]. Meanwhile, the use of the one-step global reaction model is getting increasingly popular among researchers, especially to simulate combustion in the standard Harwell furnace [15,26,27,29,30]. Magnussen and Hjertager have shown the accuracy of this model in predicting the peak of flame temperature and flame size in comparison with experimental data [31]. ANSYS Fluent supplies the interaction model called the Eddy-Dissipation Model (EDM) based on the Magnussen and Hjertager study, which has been used in this paper [31,32]. Based on the infinite fast chemistry assumptions, the eddy dissipation reaction rate depends on the turbulence behavior of the flow, and the eddy dissipation model handles the global kinetic mechanism by using a few reactions. Therefore, it is necessary to use a single step or two-step reaction for the simulation [33]. In addition, in a numerical comparison between different methane-air combustion mechanisms, Acampora et al. [34] concluded that moving from a one-step global mechanism to a two-stage global mechanism does not increase the accuracy of predictions concerning the adoption of the detailed mechanism. According to the mentioned points, the one-step global reaction for methane-air combustion has been adopted for the present simulation.

The following one-step reaction model was used for the combustion of methane-air:

$$CH_4 + 2(O_2 + 3.76N_2) \rightarrow CO_2 + 2H_2O + 7.52N_2 \tag{1}$$

The flow swirling causes the flow to move along the tangential axis in addition to the axial velocity component, which will dramatically change the fuel-air mixing rate and flame behavior. Therefore, proper simulation of flow swirl is of great importance. Due to the role of swirling in generating axial and tangential velocity components of the flow, in the present study, a dimensionless parameter of swirl number (S) in Equation (2) is used to investigate the effect of the inlet airflow swirling on the flame combustion characteristics. In this relationship, the simultaneous impact of the axial and tangential velocity components of the swirling flow is taken into account and therefore, a more accurate prediction of the swirling flow behavior can be predicted [27,35].

$$S = \frac{2}{3}\frac{v_t}{v_a} \times \left[\frac{1-\left(\frac{r_i}{r_o}\right)^3}{1-\left(\frac{r_i}{r_o}\right)^2}\right] \tag{2}$$

In the above equation $\frac{v_t}{v_a}$ is the ratio of the tangential velocity to the axial velocity of the flow, while r_i and $r_o$are respectively representing the internal and external swirl generator radius. The swirl number is calculated based on the ratio of the tangential and axial inlet airflow velocity components. Since the geometric parameters of the furnace are not changed, this ratio varies for different swirl numbers.

Table 1
Harwell furnace operational conditions.

Geometry		
Fuel inlet zone, R (mm)	0.0–6.0	
Air inlet zone, R (mm)	16.5–27.5	
Furnace diameter (mm)	150.0	
Furnace length (mm)	900.0	
Inlet boundary conditions	**Fuel**	**Air**
Axial velocity (m/s)	15.0	12.8
Radial velocity (m/s)	–	–
Swirl number	0.0	0.4
Turbulent kinetic energy (m^2/s^2)	2.26	1.63
Turbulent dissipation rate (m^2/s^3)	1131.8	692.0
Temperature (K)	295	295
Composition (mass fraction)		
Oxygen	0.0	0.2315
Nitrogen	0.0	0.7685
Methane	1.0	0.0

The interaction model namely the Eddy-Dissipation Model (EDM), based on the Magnussen and Hjertager study [31,32], has been used in this paper. The primary assumption of the model is being irreversible and one-step chemistry [36]. Along with high computing speed, the EDM model is straightforward and provides reasonable accuracy and convergence [37]. The model has also been used frequently in industrial numerical simulation of various combustion systems such as internal combustion engines [38–40], gas turbines [41–43], and furnaces [30,44,45]. The standard k-epsilon model has also been used to simulate the turbulent flow [46–49]. Due to the high temperatures in the flame, radiative heat transfer is one of the remarkable mechanisms of heat transfer from the flame [50]. Hence, its proper simulation is of great importance [51,52]. Accordingly, in the present study, the P-1 radiation model [50] has been used to model the flame heat transfer. This model is a suitable model to simulate the radiation heat transfer rate of the flame, which is widely used due to its high accuracy and ability to consider the radiation exchange between gaseous species and soot particles present in the flame environment in the simulation of combustion processes [35,53–55].

The formation of NOx is characterized by a series of strongly temperature-dependent chemical reactions known as the Zeldovich mechanism [32]. Zeldovich mechanism or thermal mechanism is one of the most understandable mechanisms to generate nitric oxide [56]. The main reactions that produce NOx from molecular nitrogen are as follows.

$$O + N_2 \leftrightarrow N + NO \tag{3}$$

$$N + O_2 \leftrightarrow O + NO \tag{4}$$

The first reaction often controls the overall reaction rate because the second reaction is much faster than the first reaction and occurs immediately after the first one [57].

To evaluate the accuracy of the results, a grid independency test was conducted on the computational domain. In this regard, the results of axial temperature distribution for 8080, 16172, 32634, 63448 nodes were compared with each other (Fig. 2a). Considering the conformity of temperature distribution for the computational grids after 16172, the solution network with 16172 nodes was selected as the best computational grid. The convergence limit was assumed when the residual values were less than10^{-6}. The calculations were performed for the four mesh sizes of 0.004100, 0.002899, 0.002040, and 0.001460 m. With the results of temperature distribution along the furnace axis, the 0.002899 m mesh size was selected for computational modeling.

3. Results and discussion

In order to validate the computational model, the numerical results of the axial temperature distribution were compared with the experimental data of Wilkes et al. [16], and the previous numerical modeling [15,29]. This comparison is presented in Fig. 2b. As shown in Fig. 2b, the presented axial temperature gradients are in good agreement with the experimental data. This figure shows that the uses of the swirl number based on the axial and tangential velocity components enhanced the resolution accuracy and made it fairly close proximity of the results to the experimental data.

Fig. 3 shows the effect of increasing the swirl number on the flow behavior. As can be seen, when the inlet flow is non-swirling (swirl number 0.0), an external recirculation zone is formed closer to the inlet of the combustion chamber. As the swirl number increases, an additional recirculation zone occurs adjacent to it, which has the opposite direction to the previous recirculation zone.

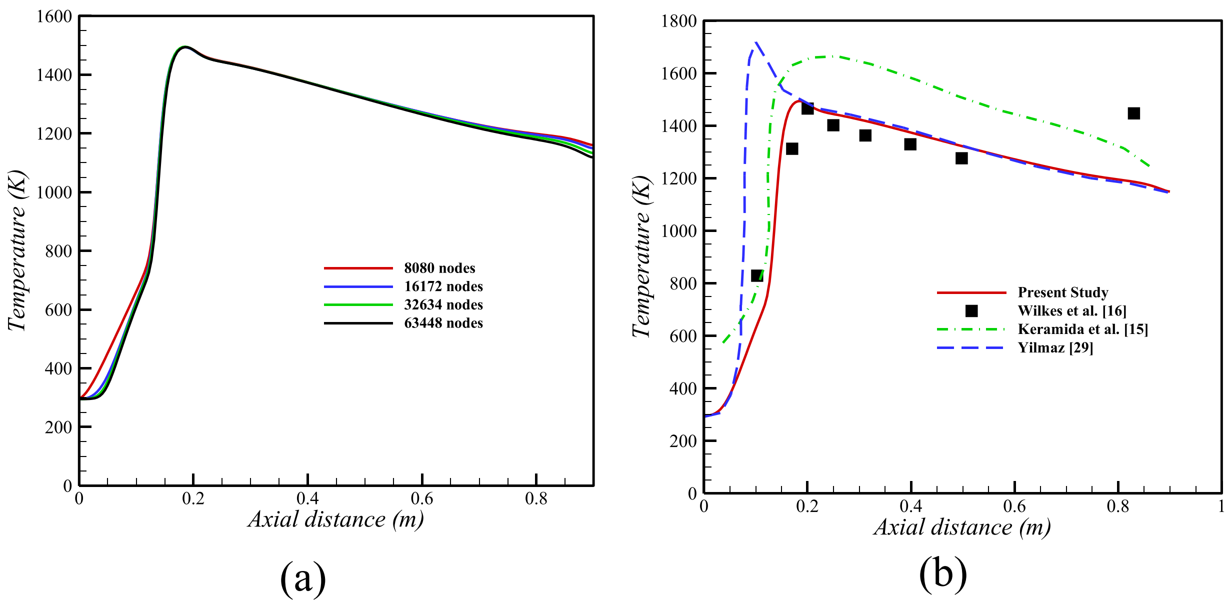

Fig. 2. (a) Grid independency test result, and (b) Validation of results.

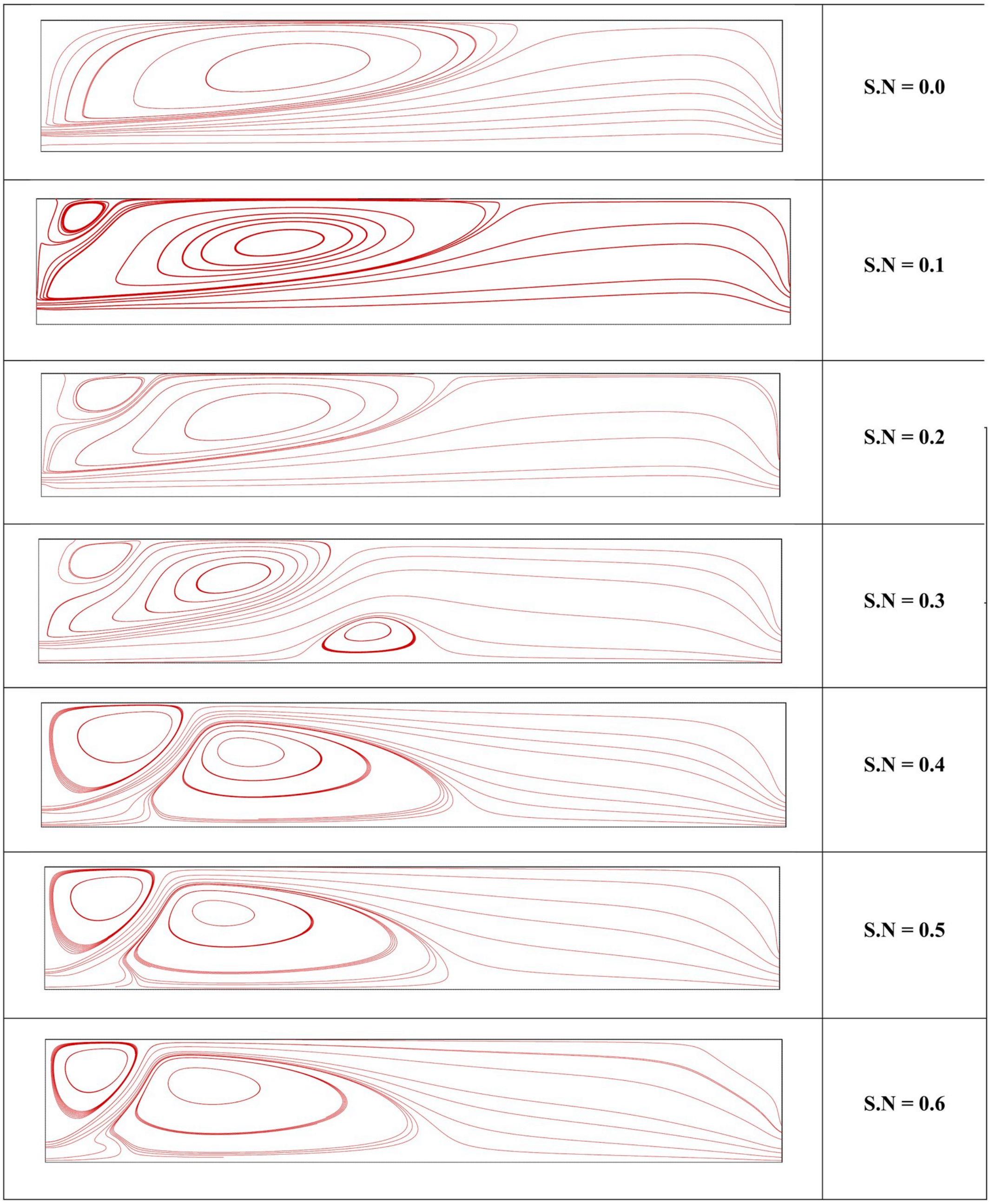

Fig. 3. Stream lines in various swirl numbers.

Further increase in the swirl number enlarge the second vortex. For instance, at swirl number 0.3, the second external recirculation zone was at its maximum size. Also, in this case, in addition to the two external recirculation zones mentioned, an internal recirculation zone begins to form in the middle of the combustion chamber. The presence of this central recirculation zone results in a better mix of fuel and oxidizer. An enhanced mix of fuel and air was formed in this area by directing the surrounding air into the flame. When the swirl number increased more than 0.3, the two external recirculation zones were combined with each other to form a single recirculation zone. Three factors including increment of the swirl number due to the enhancement of tangential flow velocity component, the deviation of the flow from the central axis of the combustion chamber, and the creation of a low-pressure zone in this region, lead to an increase in the size of the internal recirculation zone as well as a decrease in the size of the external one. The enlargement of the internal recirculation zone caused the fuel-air mixture to be drawn into the flame from longer distances and a better mix the fuel and air is generated.

Fig. 4a illustrates the axial temperature gradients for different swirl numbers, as can be seen by enhancing the swirl number due to the decrease in the axial component of the flow velocity, the location of the flame formation, and the maximum flame temperature get closer to the inlet of the combustion chamber. Approaching the flame location to the inlet of the combustion chamber causes the combustion products to have a longer residence time inside the combustion chamber and improves the rate of heat transfer from the flame. In this case, due to the radial distribution of the fuel-air mixture and the lack of fuel-air mixture concentration along the furnace axis, the maximum flame temperature also drops. Therefore, a uniform temperature distribution is created throughout the furnace. This eliminates the formation rate of Thermal NOx by eliminating the high-temperature points within the flame. Also, as shown in Fig. 4a, the temperature gradient in the swirl number 0.3 differs from the smaller and the larger swirl numbers. For swirl numbers 0.0, 0.1 and 0.2 the temperature distribution is similar to each other and its maximum location is downstream of the furnace and for swirl numbers 0.4, 0.5 and 0.6 the temperature distribution is similar, and the location of the maximum flame temperature is closer to the inlet (upstream) of the furnace. However, the swirl number 0.3 represents a transient state between the swirl numbers below and above itself, which is due to the change in the flow pattern and the vortex pattern formed in the flame, as explained in Fig. 3.

Fig. 4b illustrates the radial temperature profiles of the combustion chamber at the exhaust section (x = 0.9 m). As can be seen, by increasing the swirl number, the outlet temperature of the combustion chamber decreases, resulting in a reduction in the thermal loss. Increasing the swirl number and developing the central recirculation zone suck the combustion gases into the furnace and reduce their exhaust speed, which increase the likelihood of exchanging heat flux with the furnace wall; thereby, the exhaust temperature and the heat dissipation are reduced.

Fig. 5, illustrates the temperature distribution in the combustion chamber in the non-swirling state (swirl number 0.0) and swirl number 0.3 and 0.6. As regards the direct relation of the swirl number with the axial and tangential velocity components of the flow, it can be stated that, with the increasing of the swirl number, due to the decrease of the axial velocity component and the increase of its tangential component, the flow will spread radially, which results in a uniform temperature distribution in the combustion chamber. This uniform temperature distribution is essential in applications such as tunnel baking furnaces and improves the quality of manufactured products.

Fig. 6a illustrates the radiation heat transfer gradients along the furnace axis. Interestingly, despite decreasing mean flame temperature (Fig. 4a), as the swirl number increases, the average of radiation heat transfer from the flame enhances, which creates a uniform distribution of heat transfer flux along the furnace axis. This uniform heat distribution is very useful in industrial baking processes and makes the use of all combustion chamber space possible in these applications.

Fig. 6b shows the average radiation heat transfer flux received by the furnace wall at different swirl numbers. According to Fig. 6b, increasing the swirl number to about 0.2 does not have any significant effect on the radiant flux on the furnace wall. However, with increasing swirl number between 0.2 and 0.3, this flux enhances linearly. The reason is that no significant change in flame behavior is observed until the swirl number is less than 0.2 because of the low swirling rate; however, with increasing tangential velocity and rapid spread of the flame, the temperature distribution becomes more uniform. This uniform temperature distribution increases the flame heat exchange rate and heat flux on the furnace walls. As the swirl number goes up from 0.3 to 0.4, the radiation heat flux to the furnace wall rises slowly. At swirl number of 0.4 due to the internal recirculation zone reaching its maximum size (Fig. 3) and maximizing the fuel-air mixing rate, as well as increasing the residence time of hot combustion gases in the combustion chamber, the radiant heat transfer flux to the wall reaches its maximum value. However, for swirl numbers greater than 0.4, the radiation heat flux

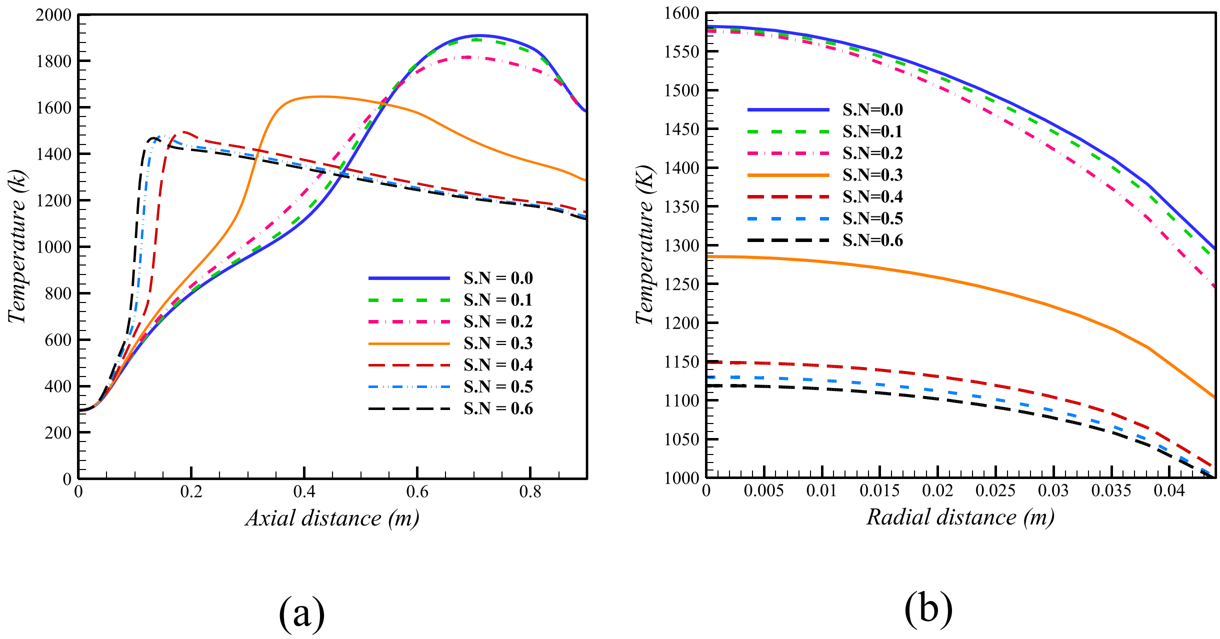

Fig. 4. Variation of (a) axial temperature, and (b) exhaust temperature at different swirl numbers.

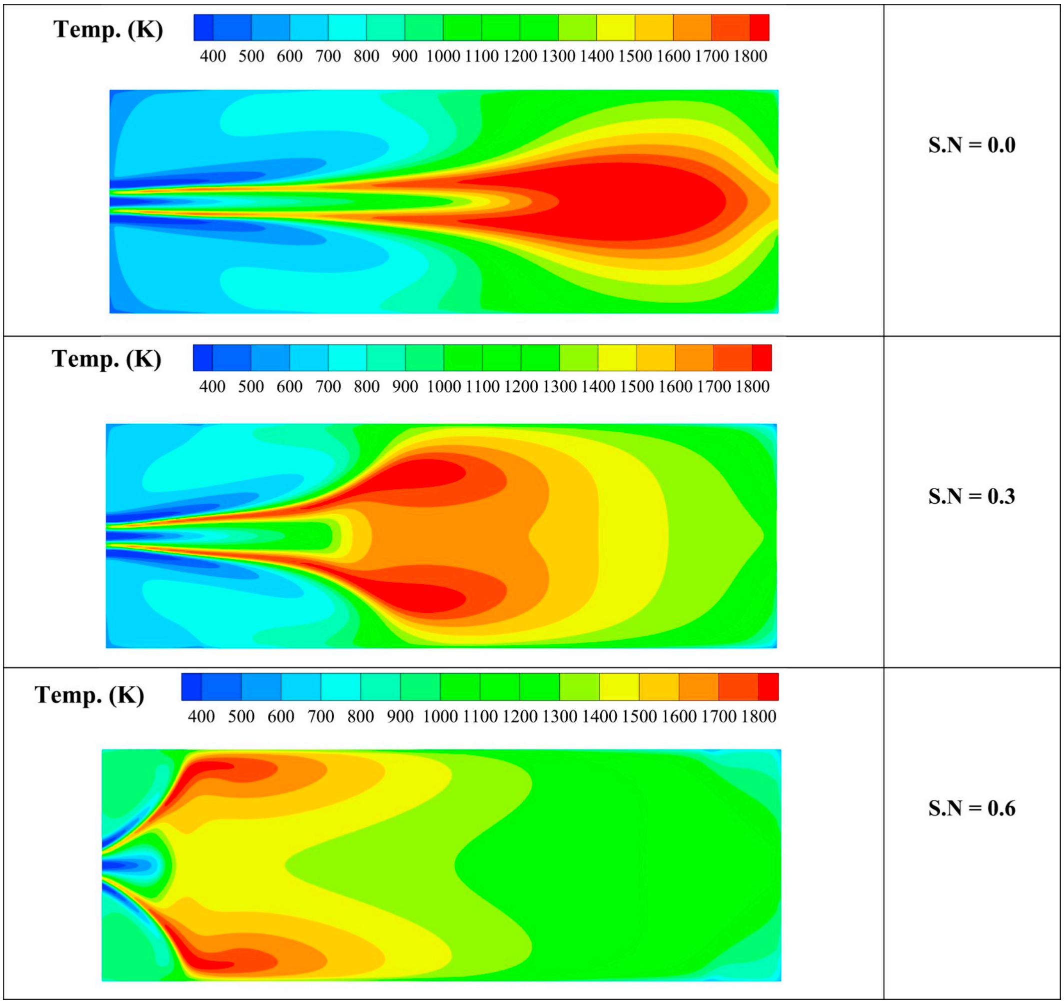

Fig. 5. Contours of temperature distribution in different swirl numbers.

remains almost constant due to the constant recirculation size.

Fig. 7a demonstrates the average distribution of NOx pollutants along the furnace axis for different swirl numbers. The rate of NOx pollutant formation is directly related to the flame temperature, the nitrogen residence time in the reacting zone, and the high-temperature zone of the flame [32,58]. Increasing the swirl number leads to a drop in the flame volume, the maximum flame temperature, and high-temperature zones (hot spot region) causing the rate of NOx formation to cut down. It is worth noting that the rate of formation of NOx in the Zeldovich thermal NOx mechanism is directly related to the flame temperature and rises exponentially with increasing the flame temperature [59]. As shown in Fig. 7a, by increasing the swirl number, the maximum NOx concentration moves from the end to the beginning of the furnace. The reason is that the maximum flame temperature is shifted towards the beginning of the furnace as the swirl number increases. Fig. 7a illustrates that the maximum amount of nitrogen oxide pollutant for the swirl numbers 0.0 to 0.2 is, much higher than that for the swirl numbers 0.3 to 0.6. The reason for this is the lack of proper fuel-air mixing for the swirl numbers between 0.0 and 0.2 and the formation of high-temperature zones in these swirl numbers. For swirl numbers between 0.3 and 0.6, due to the presence of an internal recirculation zone, the amount of this pollutant approaches the furnace inlet, and its content decreases sharply due to the perfect mixing of fuel and oxidizer and the reduction of high-temperature points in the furnace. In addition to the swirl number effect on nitrogen pollutant generation resulted from changing the gas temperature distribution mentioned above, many researchers have investigated the influence of the swirl number on the gas residence time and its impact on the NOx production rate. Chen has investigated the swirl number effect on the NOx production rate from hydrogen flames. He has found that by elevating the swirl number, the residence time and NOx generation rate reduces [60]. According to the numerical calculations carried out by Kasabov and Zarzalis [61], for a swirl-stabilized diffusion flame, it was realized that by reducing the residence time, NOx concentrations decreased significantly. Oh et al. [58] carried out an experimental study to investigate the effect of swirl flow on NOx emission in a hydrogen diffusion flame. They noticed that by increasing the swirl number, the flame length decreased, and by decreasing the flame length, due to the reduction of the reaction time between oxygen and nitrogen passing through the hot zone, the value of NOx concentration decreased.

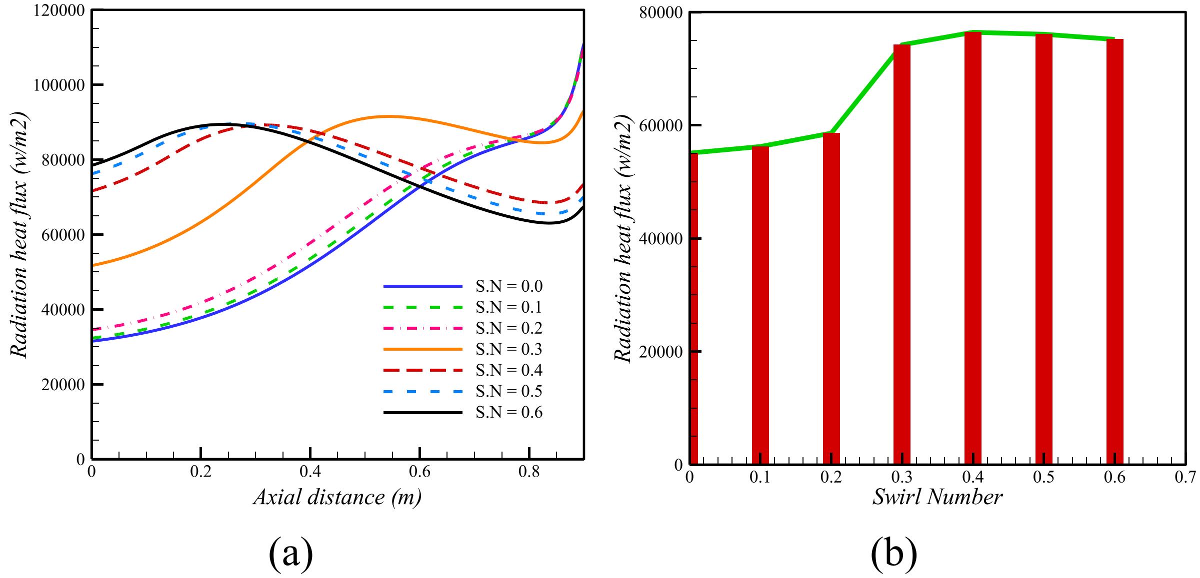

Fig. 6. Variation of (a) radiation heat transfer along the furnace axis, and (b) average of radiation heat flux on the surrounding wall at different swirl numbers.

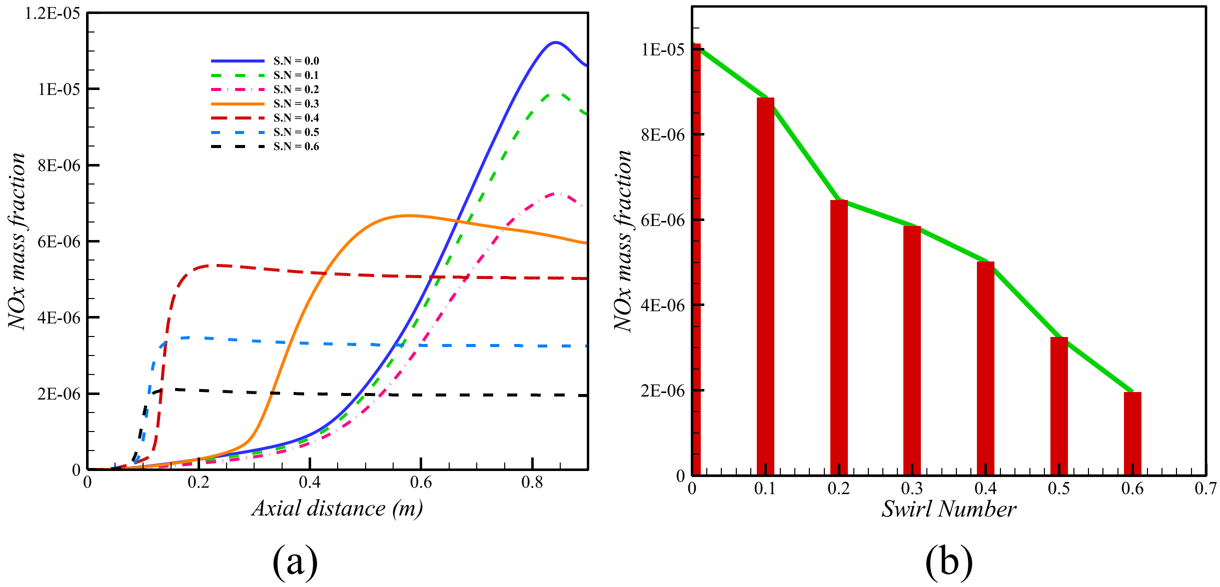

Fig. 7. NOx pollutants gradients (a) along the furnace axis, and (b) at exhaust section (x = 0.9 m) for different swirl numbers.

The NOx mass-weighted average at the exhaust section (x = 0.9 m) is calculated and reported in Fig. 7b.

As shown in Fig. 7b, increasing the swirl number reduces exhaust NOx values. This reduction can be illustrated from two perspectives. On the one hand, enhancing the swirl number results in a better fuel-air mixing rate and a decrease in high-temperature zones of the flame. Since NOx emissions are temperature-dependent pollutants, the amount of NOx generation decreases and the exhaust NOx reduces.

On the other hand, increasing the swirl number decreases the flame length. This reduction shortens the reaction time between oxygen and nitrogen in the reaction zone and eventually, produces less nitrogen oxides. As a result, the furnace exhaust NOx decreases.

4. Conclusions

In the present study, the effects of changing the inlet airflow swirl intensity on the dynamic flow behavior, temperature, and heat transfer flux of the Harwell furnace are studied using a new equation based on the tangential and axial velocity components of the flow.

The results of this study can be summarized as follows:

- By increasing the swirl number, a uniform temperature distribution throughout the furnace is generated which consequently, reduces the maximum flame temperature and eliminates high-temperature points as source formation of thermal NOx.
- Raising the swirl number increases the flame radiant heat transfer flux and generates a uniform heat flux distribution in the furnace.
- Enhancing the swirl number causes the flame to spread radially and expand the heat exchange surface area of the flame with the furnace wall.
- Increasing the swirl number while creating a uniform radial temperature distribution increases the residence time of the products in the furnace and reduces the heat loss in the chimney.
- Elevating the swirl number changes the flow pattern and creates internal and external recirculation zones in the flow.
- The role of the internal recirculation zone on the combustion behavior of the flame is much more significant than that of the external one.
- Increasing the swirl number due to the enhancement of the fuel-air mixing rate and the reduction of high-temperature concentration points significantly reduces the nitrogen oxide pollutant, which is a temperature-dependent pollutant.

The findings of the present study can be a useful and practical solution to improve the thermal efficiency of burners and to create uniform heat flux and temperature distribution in furnaces.

Declaration of competing interest

The authors declare that they have no known competing financial interests or personal relationships that could have appeared to influence the work reported in this paper.

Appendix A. Supplementary data

Supplementary data to this article can be found online at https://doi.org/10.1016/j.csite.2020.100610.

References

[1] F.A. Williams, Combustion Theory, CRC Press, 2018.
[2] N. Syred, A. Giles, J. Lewis, A. Valera Medina, P. Bowen, A. Griffiths, Tangential Velocity Effects and Correlations for Blow-Off and Flashback in a Generic Swirl Burner and the Effect of a Hydrogen Containing Fuel, 2013.
[3] Y. Tong, X. Liu, Z. Wang, M. Richter, J. Klingmann, Experimental and numerical study on bluff-body and swirl stabilized diffusion flames, Fuel 217 (2018) 352–364.
[4] L.-Y. Wang, S. Chatterjee, Q. An, A.M. Steinberg, Ö.L. Gülder, Soot formation and flame structure in swirl-stabilized turbulent non-premixed methane combustion, Combust. Flame 209 (2019) 303–312.
[5] Z. Xi, Z. Fu, X. Hu, S. Sabir, Y. Jiang, An experimental investigation on flame pulsation for a swirl non-premixed combustion, Energies 11 (7) (2018) 1757.
[6] S.S. Rashwan, The effect of Swirl number and oxidizer composition on combustion characteristics of non-premixed methane flames, Energy Fuels 32 (2) (2018) 2517–2526.
[7] H. Poorhoseinni, A. Saeedi, M. Moghiman, Experimental and numerical investigation of the inlet air swirl angle effects on temperature profile and CO, NO pollutants, Energy Engineering Management 2 (1) (2012) 32–39.
[8] L. Zhou, X. Chen, J. Zhang, Studies on the effect of swirl on no formation in methane/air turbulent combustion, Proc. Combust. Inst. 29 (2) (2002) 2235–2242.
[9] K. Bashirnezhad, M. Moghiman, M. Mousavi, On the dependence of soot formation and combustion on swirling combustion furnaces: measurement and simulation, JAST-TEHRAN- 3 (4) (2006) 205.
[10] Bonatesta, F., La Rocca, A., Shayler, P., and Wahab, E., "The Influence of Swirl Ratio on Soot Quantity and Distribution in the Cylinder of a Diesel Engine," Proc. Third European Combustion Meeting ECM.
[11] W. Jerzak, M. Kuźnia, Experimental study of impact of swirl number as well as oxygen and carbon dioxide content in natural gas combustion air on flame flashback and blow-off, J. Nat. Gas Sci. Eng. 29 (2016) 46–54.
[12] V. Patel, R. Shah, Experimental investigation on flame appearance and emission characteristics of LPG inverse diffusion flame with swirl, Appl. Therm. Eng. 137 (2018) 377–385.
[13] V. Patel, R. Shah, Effect of swirl and number of swirler vanes on combustion characteristics of methane inverse diffusion flame, J. Mech. Sci. Technol. 33 (4) (2019) 1947–1958.
[14] S. Vakilipour, Y. Tohidi, J. Al-Zaili, R. Riazi, A numerical investigation of CO 2 dilution on the thermochemical characteristics of a swirl stabilized diffusion flame, Appl. Math. Mech. (2019) 1–22.
[15] E. Keramida, H. Liakos, M. Founti, A. Boudouvis, N. Markatos, Radiative heat transfer in natural gas-fired furnaces, Int. J. Heat Mass Tran. 43 (10) (2000) 1801–1809.
[16] N. Wilkes, P. Guilbert, C. Shepherd, S. Simcox, UKAEA Atomic Energy Research Establishment, H. C. S., Div, S., UKAEA Atomic Energy Research Establishment, H. E. S. D., The Application of HARWELL-Flow3d to Combustion Problems, UKAEA Atomic Energy Research Establishment Computer Science and Systems Division, 1989.
[17] A. Khelil, H. Naji, L. Loukarfi, G. Mompean, Prediction of a high swirled natural gas diffusion flame using a PDF model, Fuel 88 (2) (2009) 374–381.
[18] K. Khanafer, S. Aithal, Fluid-dynamic and NOx computation in swirl burners, Int. J. Heat Mass Tran. 54 (23–24) (2011) 5030–5038.
[19] S. Pourhoseini, R. Nikzad, An experimental study on the effect of inlet diesel fuel temperature on mass flow choking, flame penetration, temperature, radiative characteristics and NOx pollutant emission of an oil burner, J. Braz. Soc. Mech. Sci. Eng. 41 (11) (2019) 492.
[20] C. Nayak, S.S. Sahoo, L.N. Rout, Emission analysis of a dual fuel diesel engine fuelled with different gaseous fuels generated from waste biomass, Int. J. Ambient Energy (2019) 1–6.
[21] S.H. Yoon, C.S. Lee, Experimental investigation on the combustion and exhaust emission characteristics of biogas–biodiesel dual-fuel combustion in a CI engine, Fuel Process. Technol. 92 (5) (2011) 992–1000.

[22] N.N. Mustafi, R.R. Raine, S. Verhelst, Combustion and emissions characteristics of a dual fuel engine operated on alternative gaseous fuels, Fuel 109 (2013) 669–678.
[23] J. Liu, F. Yang, H. Wang, M. Ouyang, S. Hao, Effects of pilot fuel quantity on the emissions characteristics of a CNG/diesel dual fuel engine with optimized pilot injection timing, Appl. Energy 110 (2013) 201–206.
[24] T. Boushaki, Swirling flows and flames, 2019.
[25] N. Syred, J. Beer, Combustion in swirling flows: a review, Combust. Flame 23 (2) (1974) 143–201.
[26] M.S. Skjøth-Rasmussen, O. Holm-Christensen, M. Østberg, T.S. Christensen, T. Johannessen, A. Jensen, P. Glarborg, H. Livbjerg, Post-processing of detailed chemical kinetic mechanisms onto CFD simulations, Comput. Chem. Eng. 28 (11) (2004) 2351–2361.
[27] M. İlbaş, S. Karyeyen, İ. Yilmaz, Effect of swirl number on combustion characteristics of hydrogen-containing fuels in a combustor, Int. J. Hydrogen Energy 41 (17) (2016) 7185–7191.
[28] E. Fernández-Tarrazo, A.L. Sánchez, A. Liñán, F.A. Williams, A simple one-step chemistry model for partially premixed hydrocarbon combustion, Combust. Flame 147 (1–2) (2006) 32–38.
[29] I. Yılmaz, Effect of swirl number on combustion characteristics in a natural gas diffusion flame, J. Energy Resour. Technol. 135 (4) (2013).
[30] X. Yang, Z. He, Q. Niu, S. Dong, H. Tan, Numerical analysis of turbulence radiation interaction effect on radiative heat transfer in a swirling oxyfuel furnace, Int. J. Heat Mass Tran. 141 (2019) 1227–1237.
[31] B.F. Magnussen, B.H. Hjertager, On mathematical modeling of turbulent combustion with special emphasis on soot formation and combustion, Symposium (International) on Combustion 16 (1) (1977) 719–729.
[32] A.F. Ansys, 14.0 Theory Guide, ANSYS inc, 2011, pp. 218–221.
[33] Z. Lyu, G. Li, X. Song, L. Cui, G. Ji, Z. Wang, X. Hu, Z. Xu, Comparative numerical analysis and optimization in downhole combustion chamber of thermal spallation drilling, Appl. Therm. Eng. 119 (2017) 481–489.
[34] L. Acampora, F. Marra, E. Martelli, Comparison of different CH4-Air combustion mechanisms in a perfectly stirred reactor with oscillating residence times close to extinction, Combust. Sci. Technol. 188 (4–5) (2016) 707–718.
[35] S. Karyeyen, Combustion characteristics of a non-premixed methane flame in a generated burner under distributed combustion conditions: a numerical study, Fuel 230 (2018) 163–171.
[36] Rohani, B., Wahid, M., Sies, M. M., and Saqr, K. M., "Comparison of Eddy Dissipation Model and Presumed Probability Density Function Model for Temperature Prediction in a Non-premixed Turbulent Methane Flame," Proc. AIP Conference Proceedings, American Institute of Physics, pp. 384-391.
[37] P. Wang, The model constant A of the eddy dissipation model, Progr Comput Fluid Dyn Int J 16 (2) (2016).
[38] K. Yasutomi, T. Hori, J. Senda, Simulation and Optical Diagnostics for Internal Combustion Engines," Simulations and Optical Diagnostics for Internal Combustion Engines, Springer, 2020, pp. 27–36.
[39] P. Tediya, S. Ansari, CFD Modelling and Analysis of Dual Fuel (Diesel+ Methanol) Combustion Engine with Various Blend Grade Using ANSYS (Fluent), 2018.
[40] M.R.A. Mansor, M.M. Abbood, T.I. Mohamad, The influence of varying hydrogen-methane-diesel mixture ratio on the combustion characteristics and emissions of a direct injection diesel engine, Fuel 190 (2017) 281–291.
[41] T.H. Nguyen, S. Kim, J. Park, S. Jung, S. Kim, CFD-CRN validation study for NO x emission prediction in lean premixed gas turbine combustor, J. Mech. Sci. Technol. 31 (10) (2017) 4933–4942.
[42] Kattegollahalli Shivakumar, D., Sabbani, G., Singh, G., and Harthi Revanasiddappa, P., "Prediction of Gas Turbine Afterburner Performance Using CFD for Different Operating Conditions and Reheat Strength," Proc. ASME 2017 Gas Turbine India Conference, American Society of Mechanical Engineers Digital Collection.
[43] M.A. Nemitallah, M.A. Habib, H.M. Badr, Modeling of Combustion in Gas Turbines," Oxyfuel Combustion for Clean Energy Applications, Springer, 2019, pp. 193–274.
[44] K.I. Khidr, Y.A. Eldrainy, M.M. El-Kassaby, Investigating the Potential of Different Modeling Setups in Simulating a Flameless Furnace Using Global and Detailed Kinetic Mechanisms, Combustion Science and Technology, 2019, pp. 1–35.
[45] Ma, X., Zhang, S., Yu, H., and Qi, G., "Numerical Simulation of Combustion and Emission of Blast Furnace Gas Boiler," Proc. IOP Conference Series: Materials Science and Engineering, IOP Publishing, p. 012042.
[46] Farabi, J., Ismail, M., and Abtahizadeh, E., "Simulation of Non-premixed Turbulent Natural Gas Combustion in Delft-Jet-In-Hot-Coflow Burner," Proc. 2018 International Conference on Innovation in Engineering and Technology (ICIET), IEEE, pp. 1-6.
[47] B. Kannan, S. Karthikeyan, S. Sundararaj, Comparison of Turbulence Models in Simulating Axisymmetric Jet Flow," Innovative Design and Development Practices in Aerospace and Automotive Engineering, Springer, 2017, pp. 401–407.
[48] W. Rodi, Turbulence Models and Their Application in Hydraulics, Routledge, 2017.
[49] S. Hosseini, E. Shokry, A.A. Hosseini, G. Ahmadi, J. Calautit, Evaluation of airflow and thermal comfort in buildings ventilated with wind catchers: simulation of conditions in Yazd City, Iran 35, Energy for Sustainable Development, 2016, pp. 7–24.
[50] J.R. Howell, M.P. Menguc, R. Siegel, Thermal Radiation Heat Transfer, CRC press, 2015.
[51] M. Ilbas, The effect of thermal radiation and radiation models on hydrogen–hydrocarbon combustion modelling, Int. J. Hydrogen Energy 30 (10) (2005) 1113–1126.
[52] A.A. Bhuiyan, J. Naser, Numerical modelling of oxy fuel combustion, the effect of radiative and convective heat transfer and burnout, Fuel 139 (2015) 268–284.
[53] G. Krishnamoorthy, A computationally efficient P1 radiation model for modern combustion systems utilizing pre-conditioned conjugate gradient methods, Appl. Therm. Eng. 119 (2017) 197–206.
[54] M. Wang, B. Liao, Y. Liu, S. Wang, S. Qing, A. Zhang, Numerical simulation of oxy-coal combustion in a rotary cement kiln, Appl. Therm. Eng. 103 (2016) 491–500.
[55] P. Kana-Donfack, C. Kapseu, D. Tcheukam-Toko, G. Ndong-Essengue, Numerical modeling of sugarcane bagasse combustion in sugar mill boiler, J. Energy Power Eng. 13 (2019) 80–90.
[56] Hewson, J., and Bollig, M., "Reduced Mechanisms for NOx Emissions from Hydrocarbon Diffusion Flames," Proc. Symposium (International) on Combustion, Elsevier, pp. 2171-2179.
[57] G.A. Lavoie, J.B. Heywood, J.C. Keck, Experimental and theoretical study of nitric oxide formation in internal combustion engines, Combust. Sci. Technol. 1 (4) (1970) 313–326.
[58] J. Oh, J. Hwang, Y. Yoon, EINOx scaling in a non-premixed turbulent hydrogen jet with swirled coaxial air, Int. J. Hydrogen Energy 35 (16) (2010) 8715–8722.
[59] A. Fluent, 14.5, Theory Guide, ANSYS," Inc., Canonsburg, PA, 2012.
[60] R.-H. Chen, Some characteristics of NOx emission of turbulent nonpremixed hydrogen-air flames stabilized by swirl-generated flow recirculation, Combust. Sci. Technol. 110 (1) (1995) 443–460.
[61] Kasabov, P., and Zarzalis, N., "Pressure Dependence of the Stability Limits and the NOx Exhaust Gas Concentrations in Case of Swirl-Stabilized, Diffusion Flames Burning in a Lift-Off Regime," Proc. ASME Turbo Expo 2009: Power for Land, Sea, and Air, American Society of Mechanical Engineers Digital Collection, pp. 613-622.